Catalysis Today 171 (2011) 174–179

Contents lists available at ScienceDirect

Catalysis Today

journal homepage: www.elsevier.com/locate/cattod

Preparation of supported nano-sized cobalt oxide and fcc cobalt crystallites

N. Fischer, E. van Steen, M. Claeys*

*Centre for Catalysis Research and c*change (DST-NRF Centre of Excellence in Catalysis), Department of Chemical Engineering, University of Cape Town, Cape Town 7701, South Africa*

ARTICLE INFO

Article history:
Received 31 October 2010
Received in revised form 26 February 2011
Accepted 9 March 2011
Available online 9 April 2011

Keywords:
Cobalt
Nano-crystallites
Size control
Microemulsion
Reverse micelle

ABSTRACT

In order to study the role of the crystallite size of an active phase in a catalytic reaction it is of utmost importance to be able to synthesise pure phases of crystallites in the desired size range with a narrow size distribution. In this paper we describe a new method to produce Co_3O_4 crystallites in the nanometer size range (average sizes: 3–10 nm) utilising reverse micelles as nano reactors. To prepare suitable model catalysts for studies on effects of crystallite size these crystallites can be deposited onto a variety of carriers, in this work an alumina support was used. It is further shown that the supported cobalt oxide crystallites prepared in this study do not undergo extensive sintering under reductive conditions (H_2 flow and temperatures between 375 and 450 °C) so that also a series of model catalysts with metallic cobalt crystallites of varied size could be prepared. The resulting metal phase only shows the diffraction pattern of a face-centred cubic (fcc) crystal phase, while normally mixtures of fcc an hcp cobalt were obtained in previous studies. Furthermore, almost complete reduction of the catalyst could be obtained for all crystallite sizes and no Co-aluminate formation was observed. These model catalyst systems allow the study of structure sensitive reactions with an industrially relevant catalyst system in the absence of the commonly encountered difficulties like the formation of strong metal support interactions, co-existence of different metal crystallite phases, an incomplete reducibility and crystallite growth upon exposure to reduction/reaction conditions.

1. Introduction

In recent years the interest of the scientific community in the catalytic behaviour of metal nano-crystallites has increased tremendously. With decreasing crystallite size a higher number of surface atoms per gram of the active component/metal are exposed and available for reaction. In case of surface insensitive reactions the activity per gram should therefore increase with decreasing crystallite size [1]. Studies on different systems including the CO oxidation over gold catalysts [2] or the Fischer–Tropsch synthesis over iron [3], ruthenium [4] and cobalt catalysts [5–7] show that for these systems no simple increase in activity with decreasing crystallite size exists, but that there rather is a decrease of surface specific activity, i.e. activity per active site, with decreasing crystallite size below a critical size.

The interpretation of catalytic behaviour of crystallites of different sizes can be clouded if the active phase is present in different crystal phases as it is often the case in the Fischer–Tropsch synthesis over cobalt catalysts where both fcc and hcp phases of the metal are present [8]. Ideally therefore size effects should be studied with pure crystal phases. Metallic cobalt crystallites larger than 40 nm have been reported to be stable in the hexagonal closest packed phase (hcp), while between 20 and 40 nm a mixed phase of hcp and face-centred cubic (fcc) dominates, and the fcc phase is the most stable one for sizes below 20 nm [9]. The recently described ε-cobalt only seems to be accessible via decomposition of cobalt carbonyls in solution at elevated temperatures [10]. Previous studies on the crystallite size effect of cobalt on the activity and selectivity in the Fischer–Tropsch synthesis either reported the use of mixed phases of fcc and hcp [5,11,12] or no statements were made regarding the crystallite phase [6,13].

In order to study effects of crystallite size on the activity and selectivity of catalytic reactions it is of essential need to be able to synthesise model catalysts with crystallite sizes in the nanometer range with a very narrow size distribution. Microemulsions are commonly used to produce metal or metal oxide crystallites in this size range [14,15]. In recent years the application of microemulsions as synthesis route to obtain heterogeneous catalysts has gained increasing interest ([16,17] and citations therein) with a special focus on the Fischer–Tropsch synthesis [3,4,6,12,18–21]. A microemulsion is a thermodynamically stable mixture of a surfactant, an oil phase and an aqueous phase. In the oil rich area of the ternary phase diagram, nano-sized water droplets, stabilised by a surfactant layer (in this work penta-ethyleneglycol-dodecylether (PEGDE)), form in the oil bulk phase (in this work *n*-hexane) (see Fig. 1). These structures are referred to as reverse micelles.

* Corresponding author.
E-mail address: michael.claeys@uct.ac.za (M. Claeys).

0920-5861/$ – see front matter © 2011 Elsevier B.V. All rights reserved.
doi:10.1016/j.cattod.2011.03.018

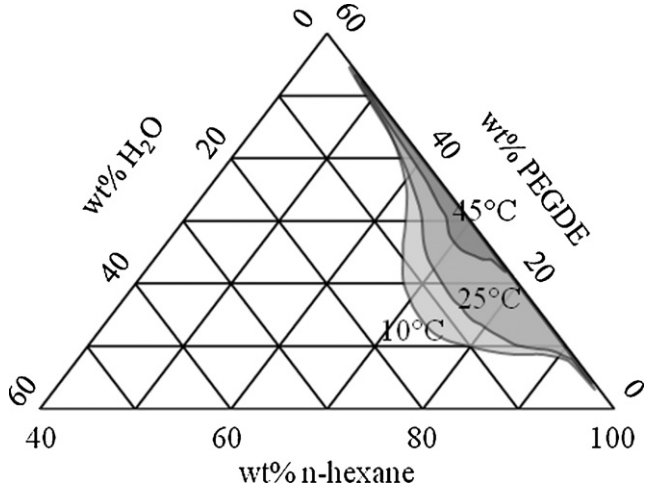

Fig. 1. Ternary phase diagram of the PEGDE, *n*-hexane and water mixture. Stability regions of reverse micelles at different temperatures are highlighted. The stability regions were determined by means of dynamic light scattering.

By dissolving metal salts in the aqueous phase, followed by precipitation or reduction, nano crystallites of the corresponding metals and metal hydroxides and oxides have been synthesised [4,6,12,15,18,20–22]. A big advantage of this synthesis method is that the size distributions of the crystallites obtained are generally very narrow, which is believed to be a consequence of the very homogeneous size distribution of the reverse micelles they originate from. It has been reported that the size of these crystallites is dependent on the size of the water droplet inside the reverse micelle [17,21,23]. This size can be "dialled" by changing the composition of the ternary system, in particular by changing the water to surfactant ratio ω [24]. With an increase in water to surfactant ratio less surfactant molecules are available to stabilise the same amount of water in the non-polar continuum. As a result the reverse micelles are reported to increase in diameter to achieve a stable w/o microemulsion [4,20]. In this study the cobalt precursor ($Co(NO_3)_2{\cdot}6H_2O$) concentration in the water core of the reverse micelle was also varied in an attempt to achieve even smaller cobalt-oxide/fcc-cobalt crystallites. Less cobalt precursor in the confined geometry of a reverse micelle would result in a decreased precipitate size and ultimately in a decrease in the size of the cobalt-oxide/fcc-cobalt crystallites.

In this article we present a novel method to produce alumina supported cobalt oxide catalysts utilising a reverse micelle method. Homogeneously sized Co_3O_4 crystallites were obtained via precipitation in microemulsions, and their sizes (average sizes: 3–10 nm) were varied via variation of the composition of the reverse micelle systems. These crystallites were then, after removal from the reverse micelle system, deposited onto an alumina support to yield a series of model catalysts with cobalt oxide crystallites of varied size. Reduction in H_2 of these model catalysts lead to a pure metallic fcc cobalt phase. Importantly, only minimal increase in crystallite size during reduction and no formation of strong cobalt–alumina interactions was observed. We are therefore able to synthesise alumina supported Co_3O_4 catalysts which can be reduced into pure fcc cobalt catalysts without any significant sintering.

2. Materials and methods

2.1. Chemicals

To prepare the supported cobalt nano crystallites the following chemicals were used: *n*-hexane and acetone supplied by KIMIX Ltd., Berol 050 (penta-ethyleneglycol-dodecylether (PEGDE)) supplied by Azko Nobel, cobalt nitrate ($Co(NO_3)_2{\cdot}6H_2O$) and 25 wt.% ammonia solution from Sigma–Aldrich. The cobalt nitrate was dried in a desiccator over silica gel prior to usage as cobalt precursor. The other chemicals were used as supplied. As the support material, commercially available alumina (Puralox, SCCa 5-150, Sasol, Germany, S_{BET} = 162 m^2/g, V_{pore} = 0.47 cm^3/g, $\bar{d}_{pore}$ = 11.5 nm, particle size = 150–200 μm) was used.

2.2. Preparation of supported cobalt nano crystallites

Berol 050 and *n*-hexane were mixed and stirred for 1 h. Cobalt nitrate solution was added drop wise and the resulting clear pink solution was stirred at 800 rpm for 2 h and left to stabilise for 12 h. No cloudiness or phase separation was observed supporting the presence of reverse micelles. Throughout the experiment the reverse micelle solutions were maintained at 25 °C in a water bath to ensure the selected w/o microemulsion compositions are in fact in the reverse micelle stability region as determined by means of dynamic light scattering (see Fig. 1). The compositions of the reverse micelle solutions used are listed in Table 1. Here the ratio of surfactant to *n*-hexane was kept constant, while the water to surfactant ratio was varied over a wider range in order to affect the size of the reverse micelle. In addition the amount/concentration of cobalt precursor ($Co(NO_3)_2{\cdot}6H_2O$) was varied to influence the size of the resulting crystallites. Precipitation of cobalt was achieved via drop wise addition of 25 wt.% ammonia solution in a molar ratio of 4:1 (NH_3 to cobalt) under stirring, resulting in a quick colour change from pink/orange to light green. The mixture was left under stirring for 30 min before 500 ml acetone was added drop wise to break up the micelle structure. The resulting green precipitate was washed extensively with acetone to remove residual surfactant, before drying over night at 120 °C in air. A calcination at 200 °C in air for 5 h yields a Co_3O_4 powder. Before its use the alumina support was calcined in a fluidised bed at 400 °C for 6 h in order to remove water and any other chemicals adsorbed during storage. 0.1 g of the obtained Co_3O_4 powder was mixed with 20 ml of distilled water in a round bottom flask. Re-suspension was achieved via ultrasonication for 2 h. The re-suspended cobalt oxide/water slurry was mixed with the corresponding amount of alumina to obtain a theoretical cobalt loading of 5 wt.%. The water was then removed under reduced pressure in a rotary evaporator to obtain the oxidic model catalysts. These catalysts were then reduced in a fixed bed under a H_2 flow (40 ml(NTP)/min/g) to prepare the reduced model catalysts (see Table 2 for details). Two different reduction temperatures were employed in order to ensure almost complete reduction of the various catalysts.

2.3. Characterization methods

The reduction behaviour of the oxidic model catalysts was studied by means of temperature programmed reduction (TPR). TPR was carried out in a Micromeritics AutoChem 2950. An amount of 100 mg of sample was heated at 10 °C/min under a flow of 5% H_2 in Ar (50 ml(NTP)/min). The exhaust gas stream was analysed by a thermal conductivity detector (TCD) to record the H_2 consumption during the reduction. The H_2 consumption was calibrated with known amounts of Ag_2O. To obtain the degree of reduction (DOR) a catalyst sample was reduced under the conditions listed in Table 2 and then further heated under 5% H_2 in Ar to 950 °C. The H_2 consumption in the latter heating step correlates to the amount of cobalt which did not reduce under the corresponding reduction conditions.

The amount of cobalt loaded was determined using atomic absorption spectroscopy (AAS) (Varian SpectraAA 110). For this, 0.05 g of catalyst was digested in a mixture of HCl/HF, HNO_3 and $HClO_3$ and then diluted in water for analysis.

Table 1
Compositions of reverse micelles for the preparation of Co_3O_4 nano crystallites.

Catalyst	*n*-Hexane (wt.%)	PEGDE (wt.%)	Co-sol.[a] (wt.%)	Conc.[b] (mol/l)	ω[c] (mol/mol)	PEGDE/n-C_6[d] (mol/mol)
CAT 9.6	83.66	11.45	4.89	0.15	8.64	33.06
CAT 8.6	84.85	11.60	3.55	0.11	6.48	33.09
CAT 6.8	85.78	11.73	2.49	0.32	8.64	33.06
CAT 5.9	87.41	11.96	0.63	0.32	4.32	33.06
CAT 4.8	87.49	11.96	0.55	0.85	1.08	33.09
CAT 4.4	85.87	11.75	2.38	0.08	1.08	33.06
CAT 4.0	86.80	11.87	1.32	0.67	4.32	33.06
CAT 3.1	87.43	11.96	0.62	0.16	2.16	33.06

[a] Cobalt solution.
[b] Concentration of $Co(NO_3)_2{\cdot}6H_2O$ in the aqueous cobalt solution.
[c] Molar water to surfactant ratio.
[d] Molar PEGDE to *n*-hexane ratio.

Table 2
Reduction temperatures and conditions for different oxidic model catalysts.

Sample	Red. temp. (°C)	Hold. time (h)	Ramp rate (°C/min)
CAT 9.6; CAT 8.6; CAT 6.8; CAT 4.0	450	6	1
CAT 5.9; CAT 4.8; CAT 4.4; CAT 3.1	375	6	1

Transmission electron microscopy (TEM) of the calcined and reduced samples was carried out on a LEO 912 OMEGA operating at 120 kV (note that reduced samples were passivated under flowing CO_2 for 1 h at room temperature). The samples were prepared using the resin method. Slices of 0.1 μm thickness were cut using a Ultramicrotome LEICA Ultracut S (Leica Microsystems). These slices were then deposited on Cu-grids and viewed at in the TEM. From the obtained images the sizes of up to 500 crystallites were measured using the freeware IMAGE J to calculate a size distribution.

High resolution TEM (HRTEM) was conducted on a FEI Tecnai F20 operating at 200 kV. Samples were suspended in ethanol and deposited on a holey carbon grid.

X-ray powder diffraction (XRD) spectroscopy was carried out in a Bruker D8 Advance laboratory X-ray diffractometer equipped with a cobalt source ($\lambda_{K\alpha1}$ = 0.178897 nm) and a position sensitive detector (VÅNTEC-2000, Bruker AXS). Unsupported Co_3O_4 as well as supported samples in their calcined state were measured as is, while reduced samples were passivated for 1 h in CO_2 prior to exposure to air. In situ measurements were carried out in a XRK-900 reaction chamber (Anton-Paar, Austria). To analyse the XRD spectra Rietveld refinement methods using TOPAS 4.2 (Bruker AXS) were applied. As the crystal structure of the alumina (predominantly consisting of γ-alumina) support is partially unknown an approach described by Scarlett and Madsen [25] for partially or not known crystal structures (PONKCS) had to be applied in order to obtain quantitative information from the XRD spectra.

3. Results and discussion

Prior to the deposition of the prepared Co_3O_4 crystallites onto the alumina support XRD patterns of the cobalt oxide powders were collected (see Fig. 2 for examples). With Rietveld refinement the composition and the different crystallite sizes as aimed for with the different microemulsion compositions could be confirmed. The desired trend as reported in the literature could be confirmed [3,4,20,23]. With a decrease in water to surfactant ratio a decreasing trend in cobalt-oxide crystallites was observed. A decrease in cobalt precursor concentration in the water core of the reverse micelle solutions also resulted in an overall decrease in the cobalt-oxide crystallite sizes (see Tables 1 and 4).

To study the reduction behaviour of the supported oxidic catalyst, temperature programme reduction was conducted (see Fig. 3). The TPR spectra show the typical reduction behaviour of cobalt oxide (Co_3O_4) displaying two mayor H_2 consumption peaks at around 250 °C and 400 °C. These two peaks can be attributed to the two reduction steps of Co_3O_4 firstly to CoO and then to metallic Co. No peaks at higher temperatures (above 600 °C) could be observed indicating the absence of strong Co–Al_2O_3 interactions (for example due to formation of $CoAl_2O_4$) [26]. The absence of these metal support interactions also allows to obtain very high degrees of reduction (i.e. almost complete reduction) at relatively mild reduction temperatures (see Table 3). Table 3 also lists the cobalt loading of the prepared catalysts. It can be noted that in nearly all cases cobalt loadings were lower that the targeted 5 wt.%,

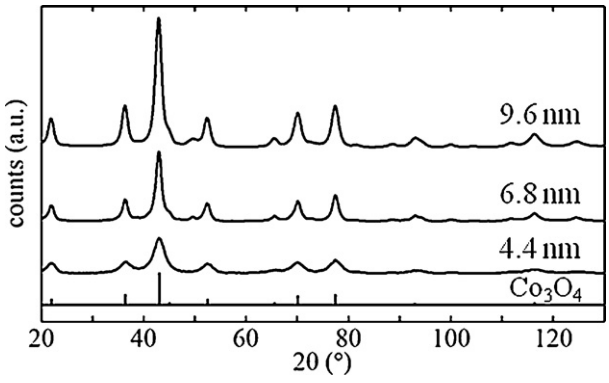

Fig. 2. XRD spectra of synthesised Co_3O_4 nano-crystallites prior to deposition onto the alumina support.

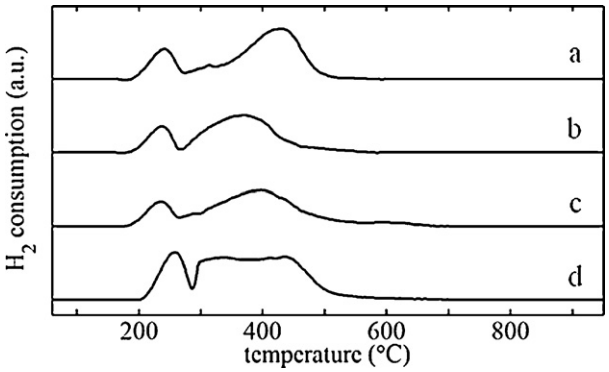

Fig. 3. TPR spectra of oxidic model catalysts ((a) CAT 4.0; (b) CAT 4.8; (c) CAT 6.8; and (d) CAT 9.6).

Table 3
Cobalt loadings and degree of reduction (DOR) of catalysts.

Sample	Co loading (wt.%)	DOR (%)
CAT 9.6	5.0	97.6
CAT 8.6	2.1	95.6
CAT 6.8	3.1	95.0
CAT 5.9	2.5	98.3
CAT 4.8	2.2	97.4
CAT 4.4	1.8	97.6
CAT 4.0	3.3	98.9
CAT 3.1	2.6	98.1

which is believed to be due to loss of the Co_3O_4 during the removal of the water of the cobalt-oxide/water slurry in the deposition step of the Co_3O_4 crystallites onto the alumina support. It was attempted to support Co_3O_4 crystallites with an average crystallite diameter of above 12 nm with the same method. The TPR spectra of these samples (data not shown) showed full reduction to metallic cobalt at temperatures below 325 °C. XRD analysis of these reduced and passivated samples indicate a high degree of sintering, with cobalt metal crystallites of approximately 50 nm. It was therefore concluded, that the preparation method as described here, does allow for deposition of cobalt-oxide crystallites of sizes smaller than the average Al_2O_3 pore size ($\bar{d}_{pore}$ = 11.5 nm) inside the alumina pores with an intimate contact with the support, but without the formation of strong metal support interaction, i.e. non reducible cobalt aluminates. This intimate contact inhibits significant crystallite growth during the reduction process as discussed below. Co_3O_4 crystallites larger than the pore diameters of the support are only loosely deposited onto the outer support surface allowing full reduction at lower temperatures but not inhibiting sintering effects.

Evaluation of the XRD spectra obtained on the oxidic catalysts confirms the presence of Co_3O_4 crystallites of different sizes (see Table 4) on the Al_2O_3 support. Reduced samples were also studied with XRD after their passivation in CO_2. Remarkably, the diffraction patterns show a pure Co (fcc) phase on the Al_2O_3 support (see Fig. 4). The average sizes of the metallic cobalt crystallites are very close to the ones obtained for the Co_3O_4 phase. This indicates that a certain amount of crystallite growth/sintering took place during reduction, as the metallic crystallites are expected to be smaller than the oxidic ones due to the loss of oxygen in the process [27].

To study the changes in crystallite phase and average size during the reduction process in situ XRD measurements were performed (see Fig. 5). At low temperatures (<200 °C) the only detectable cobalt phase on the support is the face centred cubic Co_3O_4 phase. During the course of reduction at 225 °C a rapid change in phases to the cubic Co(II)O can clearly be observed as evident by the loss of intensity of the Co_3O_4 diffraction peaks at 2θ values of 43.1°, 70.2° and 77.5° and the evolution of the diffraction pattern of Co(II)O at 2θ values of 49.7° and 72.8°. This mono oxide phase is then further reduced at temperatures of 300–350 °C to a pure fcc metallic Co

Table 4
Crystallite sizes of oxidic and reduced model catalysts, analysed via TEM and XRD.[a]

Sample	Co_3O_4 cryst. size (nm)		Co cryst. size (nm)	
	TEM[b]	XRD[a]	TEM[b]	XRD[a]
CAT 9.6	9.6 ± 1.9	10.6	10.3 ± 1.7	9.5
CAT 8.6	8.6 ± 1.3	9.5	9.5 ± 1.9	7.9
CAT 6.8	6.8 ± 1.1	6.1	6.6 ± 1.1	5.5
CAT 5.9	5.9 ± 1.1	5.3	5.6 ± 1.2	5.1
CAT 4.8	4.8 ± 1.1	4.8	5.4 ± 1.0	4.8
CAT 4.4	4.4 ± 0.9	4.4	4.5 ± 0.7	4.5
CAT 4.0	4.0 ± 0.8	4.1	4.3 ± 0.8	4.5
CAT 3.1	3.1 ± 0.8	3.6	2.9 ± 0.7	3.4

[a] Values obtained through Rietveld refinement of corresponding XRD spectra.
[b] Volume weighted mean crystallite diameters with standard deviation.

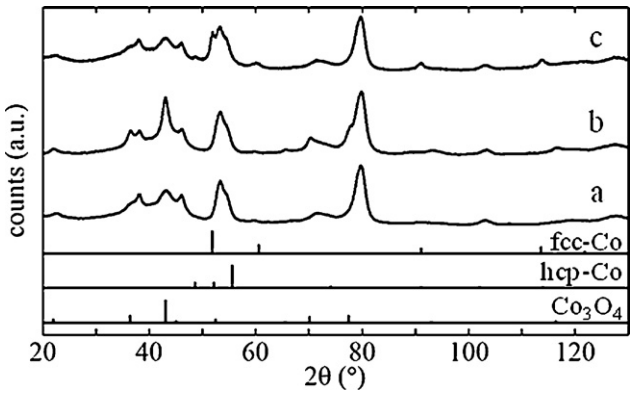

Fig. 4. XRD spectra of (a) Al_2O_3; (b) CAT 9.6 in oxidic state; and (c) CAT 9.6 reduced in H_2 and passivated in CO_2.

phase (2θ = 51.8° and 91.1°). Rietveld refinement indicates that no other phase than the metallic fcc cobalt phase is present after the reduction. This corresponds well with the high degrees of reduction obtained via TPR measurements (see Table 3). It is remarkable to note that no hcp cobalt phase could be detected in the reduced catalyst. The fcc cobalt phase is the stable conformation at high temperatures. Several studies have shown that the hcp cobalt phase can be converted into a fcc phase at temperatures of 500 °C in the presence of hydrogen for crystallites in the micrometer size range [28–30]. Kitakami et al. [9] report a crystallite size dependency of the stable cobalt phase, with crystallites below a diameter of 20 nm being stable in the fcc conformation. Previous studies on nano-sized cobalt crystallites, however, reported the presence of a mixed phase of fcc and hcp [5,11] or no statements were made regarding the crystallite phase [6,13]. It may be speculated that the combination of high reduction temperature, especially in the second reduction step from Co(II)O to metallic cobalt, and small crystallite size results in the pure fcc cobalt phase observed in this study.

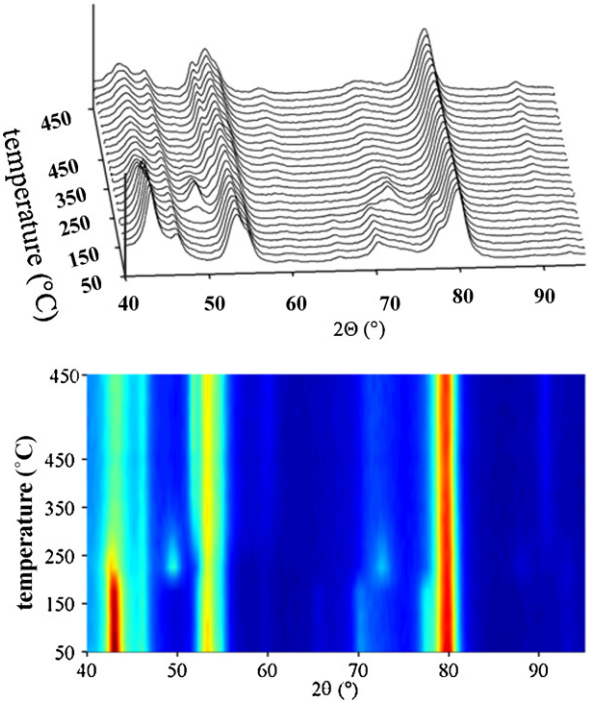

Fig. 5. In situ XRD reduction of catalyst CAT 9.6 (reduction conditions: 6 h at 450 °C under 40 ml(NTP)/min/g H_2, ramp rate 1 °C/min); *top* diffraction patterns, *bottom* on top view.

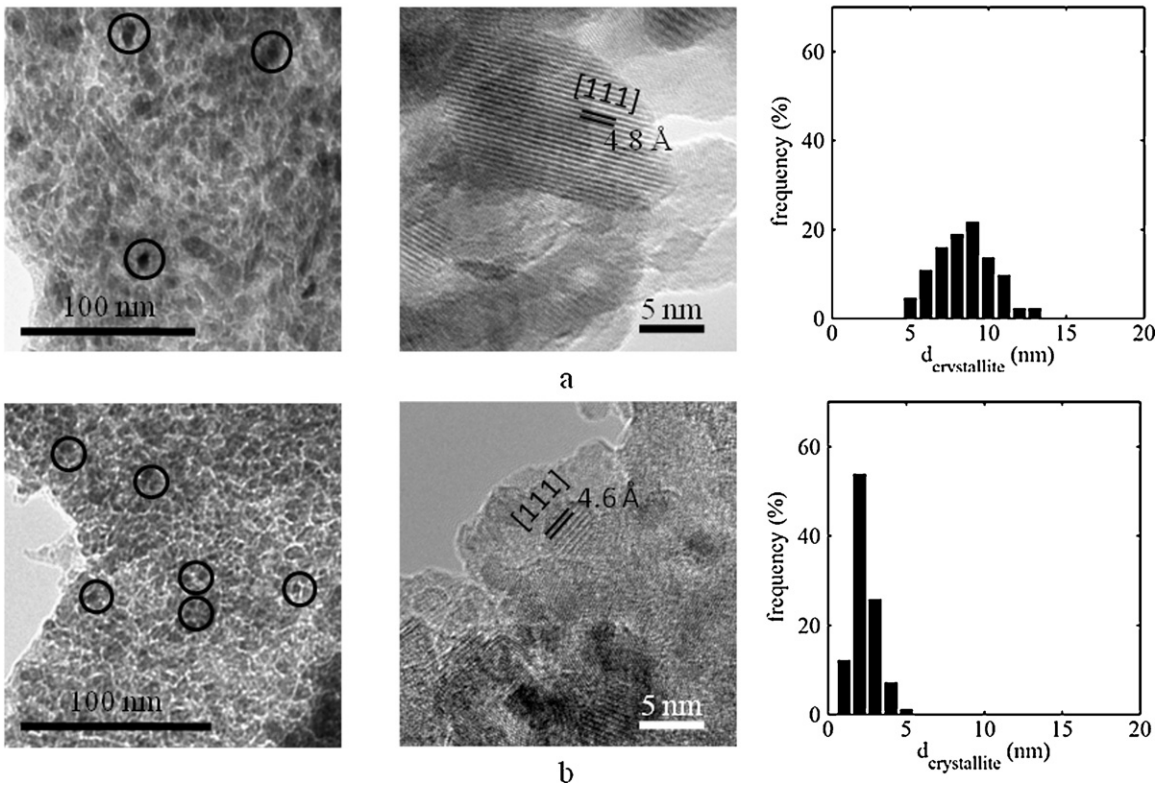

Fig. 6. TEM (magnification = 60k) and HRTEM (magnification = 700k) micrographs of (a) CAT 9.6 in calcined state with corresponding crystallite size distribution and (b) CAT 3.1 in calcined state with corresponding crystallite size distribution. Co_3O_4 crystallites in the TEM micrographs are encircled.

From TEM pictures, the size distributions of the cobalt crystallites, in their oxidic and reduced states, were measured (see Table 4 and Fig. 6). In all cases the sizes show a very narrow distribution indicated by the small value of the standard deviation (σ). The size difference between the calcined oxidic and the reduced metallic samples is very low. In the literature the size of the reduced crystallite is often assumed to be three quarters the size of the metal oxide due to the loss of the oxygen atoms during reduction [12,18,27]. The absence of this decrease in size of the cobalt crystallites can be explained with slight crystallite growth due to sintering effects which are enhanced in the presence of water forming during the reduction [31]. However, the observed crystallite growth is not severe so that the model characteristics of the catalysts could be maintained and a series of nano sized metallic cobalt crystallites with narrow size distributions on the alumina support were obtained. The average sizes obtained from TEM analyses cor-

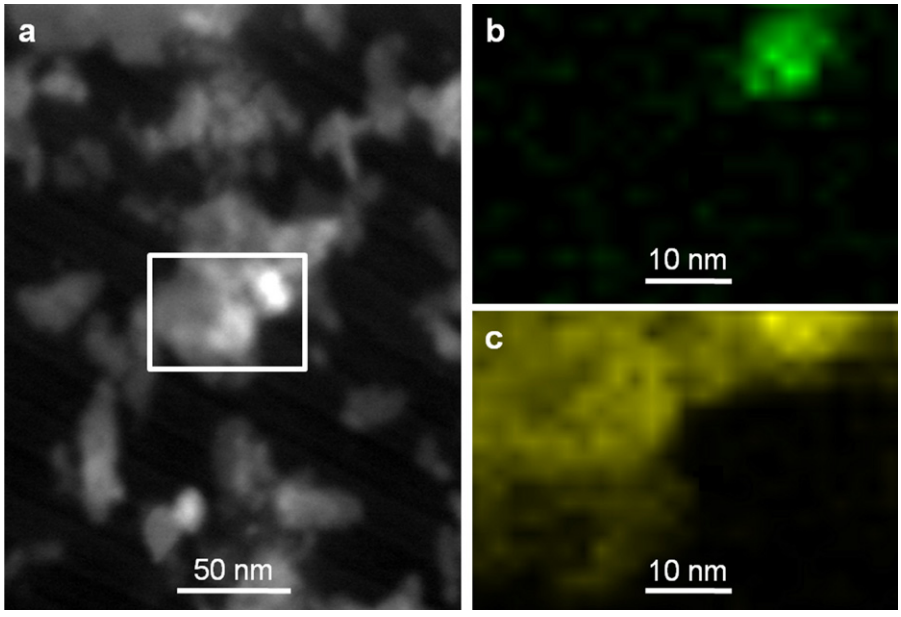

Fig. 7. EDX maps of STEM micrograph of CAT 9.6 in calcined state: (a) STEM micrograph; (b) cobalt map of boxed area in (a); and (c) aluminium map of boxed area in (a).

respond well with the results obtained from the XRD studies (see Table 4). For this volume weighted mean crystallite diameters were calculated from the TEM analyses.

The identification of cobalt phases on an alumina support with transmission electron microscopy methods is problematic due to their similar densities. To identify and confirm the Co_3O_4 phase, the lattice parameters of crystalline structures obtained with HRTEM were compared to values reported in the literature (4.7 Å [32]) and to values obtained from pure cobalt phases in the absence of alumina support. Generally a very good agreement could be found (see Fig. 6). HRTEM images of the reduced and passivated cobalt catalysts showed the same crystal lattices as calcined samples. It is therefore assumed, that the reduced and passivated model catalyst samples did undergo re-oxidation prior to the analysis by HRTEM. Cobalt and alumina rich areas in the micrographs were furthermore identified by means of energy-dispersive X-ray spectroscopy (EDX) maps of scanning TEM (STEM) (see Fig. 7).

4. Conclusions

In this article we present a novel method utilising reverse micelles to prepare homogeneous cobalt nano crystallites of varied average size, which have been supported on a commercially available Al_2O_3 to yield a series of oxidic model catalysts with varied cobalt oxide crystallite size (3–10 nm). Importantly the size of these crystallites could be maintained upon reductive treatment in hydrogen, so that also a series of reduced catalysts with varied cobalt crystallite size could be obtained. Remarkably, almost complete reduction could be obtained and the metallic phase formed was fcc cobalt only. These catalysts, both oxidic and reduced, are therefore ideal model systems to study size dependencies in suitable catalytic reactions.

Acknowledgements

The authors thank the Centre for Catalysis Research at the Department of Chemical Engineering of the University of Cape Town and c*change (DST-NRF Centre of Excellence in Catalysis) for their financial support during the course of this work.

The authors would also like to acknowledge the help and contributions from Mrs. H. Divey and Mrs. S. Vasic with the AAS measurements, Mr. M. Jaffer from the Electron Microscope Unit at the University of Cape Town with the TEM and the HRTEM instruments, Mr. F. Koch from the Electron Microscope Unit at the University of the Western Cape with the EDX scans and Mr. B. Clapham and Mr. C. Shilubane for the mapping of the stability region of the reverse micelle system at different temperatures.

References

[1] M. Boudart, M.A. McDonald, Journal of Physical Chemistry 88 (1984) 2185.
[2] M. Haruta, Catalysis Today 36 (1997) 153.
[3] E.I. Mabaso, E. van Steen, M. Claeys, DGMK/SCI-Conference "Synthesis Gas Chemistry", 2006.
[4] C.A. Welker, Ruthenium based Fischer–Tropsch Synthesis on Crystallites and Clusters of Different Sizes, vol. PhD, University of Cape Town, 2007.
[5] G.L. Bezemer, J.H. Bitter, P.C.E. Kuipers Herman, H. Oosterbeek, J.E. Holewijn, X. Xu, F. Kapteijn, A.J. van Dillen, K.P. de Jong, Journal of the American Chemical Society 128 (2006) 3956.
[6] G. Prieto, A. Martínez, P. Concepción, R. Moreno-Tost, Journal of Catalysis 266 (2009) 129.
[7] Ø. Borg, P.D.C. Dietzel, A.I. Spjelkavik, E.Z. Tveten, J.C. Walmsley, S. Diplas, S. Eri, A. Holmen, E. Rytter, Journal of Catalysis 259 (2008) 161.
[8] H. Karaca, J. Hong, P. Fongarland, P. Roussel, A. Griboval-Constant, M. Lacroix, K. Hortmann, O.V. Safonova, A.Y. Khodakov, Chemical Communications (Cambridge, U.K.), 46(2010)788.
[9] O. Kitakami, H. Sato, Y. Shimada, F. Sato, M. Tanaka, Physical Review B: Condensed Matter 56 (1997) 13849.
[10] D.P. Dinega, M.G. Bawendi, Angewandte Chemie International Edition 38 (1999) 1788.
[11] D.I. Enache, B. Rebours, M. Roy-Auberger, R. Revel, Journal of Catalysis 205 (2002) 346.
[12] A. Martinez, G. Prieto, Catalysis Communications 8 (2007) 1479.
[13] S.W. Ho, M. Houalla, D.M. Hercules, Journal of Physical Chemistry 94 (1990) 6396.
[14] V. Uskokovic, M. Drofenik, Surface Review and Letters 12 (2005) 239.
[15] M.P. Pileni, Journal of Physical Chemistry 97 (1993) 6961.
[16] M. Boutonnet, S. Lögdberg, E. Elm Svensson, Current Opinion in Colloid & Interface Science 13 (2008) 270.
[17] S. Eriksson, U. Nylen, S. Rojas, M. Boutonnet, Applied Catalysis A: General 265 (2004) 207.
[18] A. Martinez, G. Prieto, Journal of Catalysis 245 (2007) 470.
[19] V. Cheang, Effect of Crystallite Size and Water Partial Pressure on thr Activity and Selectivity of Low Temperature Iron-based Fischer–Tropsch Catalysts, vol. PhD, Department of Chemical Engineering, University of Cape Town, Cape Town, 2009, p. 285.
[20] D. Barkhuizen, I. Mabaso, E. Viljoen, C. Welker, M. Claeys, E. van Steen, J.C.Q. Fletcher, Pure Applied Chemistry 78 (2006) 1759.
[21] E.I. Mabaso, Nanosized Iron Crystallites for Fischer–Tropsch Synthesis, vol. PhD, University of Cape Town, Cape Town, 2005.
[22] M. Ojeda, S. Rojas, M. Boutonnet, F.J. Pérez-Alonso, F. Javier García-García, J.L.G. Fierro, Applied Catalysis A: General 274 (2004) 33.
[23] I. Lisiecki, Journal of Physical Chemistry 109 (2005) 12231.
[24] T. Kinugasa, A. Kondo, S. Nishimura, Y. Miyauchi, Y. Nishii, K. Watanabe, H. Takeuchi, Colloids and Surfaces A: Physicochemical and Engineering Aspects 204 (2002) 193.
[25] N.V.Y. Scarlett, I.C. Madsen, Powder Diffraction 21 (2006) 278.
[26] A. Sirijaruphan, A. Horvath, J.G. Goodwin Jr., R. Oukaci, Catalysis Letters 91 (2003) 89.
[27] D. Schanke, S. Vada, E.A. Blekkan, A.M. Hilmen, A. Hoff, A. Holmen, Journal of Catalysis 156 (1995) 85.
[28] J. Ahmed, S. Sharma, K.V. Ramanujachary, S.E. Lofland, A.K. Ganguli, Journal of Colloid and Interface Science 336 (2009) 814.
[29] J.E. Bidaux, R. Schaller, W. Benoit, Acta Metallurgica 37 (1989) 803.
[30] R. Speight, A. Wong, P. Ellis, P.T. Bishop, T.I. Hyde, T.J. Bastow, M.E. Smith, Physical Review B: Condensed Matter and Materials Physics 79 (2009) 054102/1.
[31] G. Jacobs, P.M. Patterson, Y. Zhang, T. Das, J. Li, B.H. Davis, Applied Catalysis A: General 233 (2002) 215.
[32] Z. Hui, W. Jinbo, Z. Chuanxin, M. Xiangyang, D. Ning, T. Jiangping, Y. Deren, Nanotechnology 19 (2008) 035711.